Replication stress induces tumor-like microdeletions in *FHIT*/FRA3B

Sandra G. Durkin*, Ryan L. Ragland*, Martin F. Arlt*, Jennifer G. Mulle†, Stephen T. Warren†, and Thomas W. Glover*‡

*Department of Human Genetics, University of Michigan, Ann Arbor, MI 48109-5618; and †Department of Human Genetics, Emory University, Atlanta, GA 30322

Edited by Philip C. Hanawalt, Stanford University, Stanford, CA, and approved November 12, 2007 (received for review August 27, 2007)

Common fragile sites (CFSs) are loci that preferentially exhibit metaphase chromosome gaps and breaks after partial inhibition of DNA synthesis. The fragile site FRA3B, which lies within the *FHIT* tumor-suppressor gene, is a site of frequent heterozygous and homozygous deletions in many cancer cells and precancerous lesions. The great majority of *FHIT* and other CFS-associated gene rearrangements in tumors are submicroscopic, intralocus deletions of hundreds of kilobases that often result in inactivation of associated genes. Although CFS instability leads to chromosome gaps and breaks and translocations, there has been no direct evidence showing that CFS instability or replication stress can generate large submicroscopic deletions of the type seen in cancer cells. Here, we have produced FHIT/FRA3B deletions closely resembling those in tumors by exposing human–mouse chromosome 3 somatic hybrid cells to aphidicolin-mediated replication stress. Clonal cell populations were analyzed for deletions by using PCR, array comparative genomic hybridization (aCGH), and FISH. Thirteen percent to 23% of clones exhibited submicroscopic *FHIT* deletions spanning ≈200–600 kb within FRA3B. Chromosomes with FRA3B deletions exhibited significantly decreased fragility of this locus, with a 2- to 12-fold reduction in metaphase gaps and breaks compared with controls. Sequence analysis showed no regions of homology at breakpoints and suggests involvement of NHEJ in generating the deletions. Our results demonstrate that replication stress induces a remarkably high frequency of tumor-like microdeletions that reduce fragility at a CFS in cultured cells and suggests that similar conditions during tumor formation lead to intralocus deletion and inactivation of genes at CFSs and perhaps elsewhere in the genome.

fragile site | genome instability | replication stress

Common fragile sites (CFSs) are regions of the genome that are particularly susceptible to forming gaps and breaks on metaphase chromosomes under conditions of replication stress induced by certain inhibitors of DNA synthesis, particularly the polymerase-inhibiting drug, aphidicolin (APH) (1, 2). The ATR-dependent DNA damage checkpoint has been shown to be centrally involved in maintenance of CFS stability, leading to the model that CFS lesions result from stalled replication at these sites (3–6).

In addition to cytogenetic "expression" of CFS gaps and breaks on metaphase chromosomes, CFSs exhibit a number of additional characteristics of unstable DNA in cultured cells. After induction with APH, the majority of CFS breaks display sister chromatid exchanges (SCEs) (7). Chromosome breakage at CFSs can lead to translocations and gross chromosome terminal deletions after APH treatment in somatic cell hybrid systems in which there is no negative selection for loss of genes distal to the CFS (8, 9). CFSs are also preferred sites of integration for transfected DNA in cells pretreated with APH (10–12) and have been implicated in breakage leading to intrachromosomal gene amplification events in cultured CHO cells (13).

Although normally stable in most somatic cells *in vivo*, numerous studies have shown that CFSs are sites of frequent chromosome breakage and rearrangements in cancer cells. The CFS-specific rearrangements most frequently observed are one or more submicroscopic deletions of several hundred kilobases directly within the CFS region, often resulting in inactivation of the associated genes (reviewed in refs. 14 and 15). Most such studies have focused on FRA3B and FRA16D because they are the two most frequently expressed and best-characterized CFSs, and both lie within the large tumor-suppressor genes, *FHIT* and *WWOX*, respectively (16, 17).

FRA3B is the most fragile site in the genome and extends over >500 kb within the 1.5-Mb *FHIT* gene (16, 18, 19). Consistent with its proposed function as a tumor suppressor, homozygous genomic deletions within the *FHIT* gene have been observed in a large number of human cancers and cancer cell lines, including lung, breast, gastric, cervical, and esophageal carcinomas (reviewed in ref. 20). Rearrangements of the short arm of chromosome 3, especially within *FHIT*, are among the most frequently acquired genetic changes in lung pathogenesis (21–23). For example, Li *et al.* (22) observed 79% of 38 non-small-cell lung cancer (NSCLC) tumors had deletions in *FHIT*. In addition, deletion breakpoints in FRA3B and other CFSs have been shown to occur in precancerous lesions in association with activated DNA damage checkpoints (24, 25) and in the earliest stages of esophageal adenocarcinoma (26). The discontinuous nature of a number of deletions within FRA3B in tumor cell lines has been suggested as evidence of ongoing instability in CFS regions (21). Although submicroscopic deletions within CFSs in cancer cells are common, many fewer translocations or cytological detectable gross deletions, such as those exhibited in cultured cells (8), have been reported (reviewed in ref. 20).

It has been assumed that the mechanism leading to these submicroscopic deletions in *FHIT* and other CFS genes in tumor cells is CFS instability after replication stress. However, there is no direct experimental evidence from studies of mammalian cells or cells from any organism that either CFS breakage or replication stress can lead to frequent deletions of hundreds of kilobases as seen in tumor cells. Based on the knowledge that APH is known to induce translocations and other gross chromosomal rearrangements with breaks at CFSs in hamster–human somatic cell hybrids (8) we hypothesized that tumor-like submicroscopic deletions at CFSs would be induced and could be detected in a modified experimental system using high-resolution genome analysis.

In experiments described here, human–mouse chromosome 3 somatic cell hybrid cells were subjected to replication stress through low-dose APH treatment to induce CFS lesions. Multiplexed PCR markers spanning FRA3B were used to detect deletions within *FHIT*/FRA3B. We observed *FHIT*/FRA3B deletions spanning

Author contributions: S.G.D., M.F.A., and T.W.G. designed research; S.G.D., R.L.R., J.G.M., and T.W.G. performed research; S.G.D., J.G.M., S.T.W., and T.W.G. contributed new reagents/analytic tools; S.G.D., R.L.R., M.F.A., J.G.M., S.T.W., and T.W.G. analyzed data; and S.G.D., R.L.R., M.F.A., J.G.M., S.T.W., and T.W.G. wrote the paper.

The authors declare no conflict of interest.

This article is a PNAS Direct Submission.

‡To whom correspondence should be addressed at: Department of Human Genetics, University of Michigan, 4909 Buhl, Box 0618, 1241 East Catherine Street, Ann Arbor, MI 48109-5618. E-mail: glover@umich.edu.

This article contains supporting information online at www.pnas.org/cgi/content/full/0708097105/DC1.

Table 1. Proportion of clones with deletions in FRA3B

APH dose, μM	Frequency of clones with FRA3B deletions, %	No. of clones with FRA3B deletions	*P*, compared with control
0.0	0	0/30	—
0.3	13	4/30	0.112
0.6	23	7/30	0.011
Total	18	11/60	0.013

hundreds of kilobases that closely resembled those found in tumors at a remarkably high frequency in isolated cell clones. Clones with intralocus FRA3B deletions showed a significant reduction in FRA3B breaks on metaphase chromosomes. Our results demonstrate that replication stress induces a high frequency of tumor-like submicroscopic deletions of hundreds of kilobases within *FHIT*/FRA3B and suggests that similar conditions during tumor formation leads to intralocus deletion and inactivation of genes at CFSs and perhaps elsewhere in the genome.

Results

Identification of Submicroscopic Deletions Within *FHIT*/FRA3B. A somatic human–mouse hybrid cell model system was used to examine the effects of APH-mediated replication stress on inducing deletions within *FHIT*/FRA3B. A subclone of a chromosome 3 human–mouse somatic cell hybrid cell line (GM11713A) with a G418-resistance (neo^r) selectable marker gene inserted at 3p21.3 (distal to FRA3B at 3p14.2) was used in these experiments (27). The location of the neo^r gene was verified by inverse PCR (data not shown). GM11713A cells contain a single copy of human chromosome 3, including an intact FRA3B region, in addition to a full complement of the mouse genome. Therefore, rearrangements of chromosome 3 that do not result in loss of the neo^r gene should not be selected against in culture.

Because GM11713A cells are hemizygous for human chromosome 3, FRA3B deletion screening was performed by PCR. One hundred forty-six PCR markers spaced at ≈10- to 30-kb intervals were designed spanning the entire 1.5-Mb *FHIT* gene and 3 Mb of flanking sequence [supporting information (SI) Table 4]. Thirty clones derived from treatment with each of two APH doses and 30 untreated clones were screened for deletions (90 total). Primers were multiplexed so that each reaction was internally controlled with a positive PCR result. We found that 4 of 30 (13%) clones treated with 0.3 μM APH exhibited deletions in FRA3B (P = 0.112). Seven of 30 (23%) clones treated with 0.6 μM APH exhibited deletions in FRA3B, a significantly higher percentage than the untreated control group (P = 0.011), which did not exhibit any deletions (Table 1). The higher frequency of deletions observed in cells treated with 0.6 μM APH compared with cells treated with 0.3 μM APH is indicative of a dose-dependent response. In total, 11 clones with FRA3B deletions were isolated, representing a combined frequency of 18%. It is possible that this is an underestimate of the actual frequency of induced deletions, because plating efficiency of APH-treated cells was decreased compared with untreated cells (SI Fig. 6).

All 11 clones had deletions that completely lie within the boundaries of *FHIT*, and most deletions centered on exon 5 of *FHIT*, which is considered the center of FRA3B fragility (Fig. 1). The average deletion size was ≈392 kb, with the smallest and largest deletions spanning ≈187.2 and 618.8 kb, respectively (Table 2). Clones generated with 0.3 μM APH had an average deletion size of ≈359.3 kb, whereas those generated at 0.6 μM APH had a slightly larger average deletion size of ≈411.3 kb. In general, deletions extend from *FHIT* intron 3 to intron 5, and each deletion was unique. Four additional clones with FRA3B deletions induced by 0.6 μM APH treatment were generated in a smaller pilot experiment (clones *p*-10, *p*-43, *p*-154, and *p*-851) and were characterized by PCR but not included in frequency analysis of APH-induced deletions, for a total of 15 deletion clones (Fig. 1).

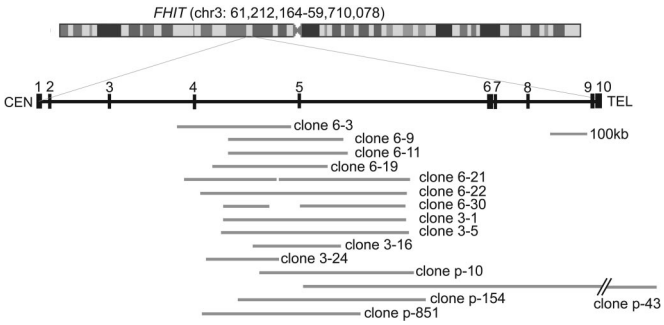

Fig. 1. Map of APH-induced *FHIT*/FRA3B deletions. PCR-mapped positions of APH-induced deletions in *FHIT*/*FRA3B* in hybrid clones. Clones 6-3, 6-9, 6-11, 6-19, 6-21, 6-22, 6-30, *p*-10, *p*-43, *p*-154, and *p*-851 were derived from treatment with 0.6 mM APH. Clones 3-1, 3-5, 3-16, and 3-24 were derived from treatment with 0.3 mM APH.

Confirmation of Deletions by FISH and Array Comparative Genomic Hybridization (aCGH). All 15 *FHIT*/FRA3B deletions identified by PCR were verified by FISH analysis. A control fosmid mapping outside of the deletions (WIBR2-2244H18) and a test fosmid (WIBR2-1521A22 or WIBR2-1588A06) from within the deleted regions were used as FISH probes and hybridized to metaphase preparations from deletion clones. All clones with suspected *FHIT*/FRA3B deletions hybridized the control probe, but not the test probe (SI Fig. 7).

To further confirm deletions and to increase resolution of deletion boundaries, four deletion clones (3-16, 6-30, *p*-43 and *p*-851) were selected for aCGH analysis using high-density microarrays containing oligonucleotides spaced at 110-bp intervals spanning the *FHIT* locus (Fig. 2). The aCGH-detected breakpoints fell within the predicted deletion boundaries determined by PCR, except for clone *p*-43, which was found to have a distal breakpoint falling ≈2 Mb further telomeric than the PCR detected distal breakpoint (Tables 2 and 3). This discrepancy was based on the result of a positive PCR signal with a single PCR primer pair and therefore is most likely a result of PCR artifact or a complex rearrangement in this clone. Interestingly, one of four clones analyzed by aCGH, clone 3-16, showed a 50-kb duplication neighboring the ≈230-kb deletion in FRA3B (Fig. 2 and Table 3), suggesting that APH-mediated replication stress can induce large duplications in addition to deletions.

APH-Induced Deletions Within *FHIT* Resemble Those Found in Cancer. Several groups have mapped homozygous deletions within FRA3B in various tumors and tumor-derived cell lines by using markers in each of the *FHIT* exons (16, 23, 28, 29). We compared a number of these *FHIT* deletions reported in the literature with our APH-induced deletions (Fig. 3). Although the resolution of the tumor breakpoints is, in general, much lower than for our deletion clones, the APH-induced deletions resemble the size of and coincide with or span many of these tumor deletions. For example, esophageal cancer cell lines, small-cell lung carcinomas, non-small-cell lung carcinomas, and breast cancers, like the hybrid deletion clones, have deletions centered around *FHIT* exon 5 (22, 28, 29).

Deletions Within *FHIT*/FRA3B Significantly Reduce CFS Instability. To determine the effects of deletions on FRA3B fragility, seven clones with unique deletions were analyzed for APH-induced gaps and breaks on metaphase chromosomes (Fig. 4). Seventy-five metaphases were scored for FRA3B breakage in each of the seven

GENETICS

Table 2. Deletion breakpoint regions determined by PCR

Clone	Chr. 3 distal breakpoint position (size, bp)	Chr. 3 proximal breakpoint position (size, bp)	Deletion size range, kb
3-1	60,206,616–60,202,204 (4,412)	60,710,149–60,702,855 (7,294)	496.2–507.9
3-5	60,202,369–60,198,628 (741)	60,714,271–60,709,997 (4,851)	507.6–515.6
3-16	60,402,073–60,391,764 (10,309)	60,630,221–60,626,399 (3,822)	224.3–238.5
3-24	60,566,383–60,561,053 (5,330)	60,758,476–60,753,625 (4,851)	187.2–197.2
6-3	60,539,566–60,533,393 (6,173)	60,842,259–60,838,199 (4,060)	298.6–308.9
6-9	60,392,607–60,385,946 (6,661)	60,702,855–60,697,398 (5,457)	310.2–311.5
6-11	60,379,475–60,373,686 (5,798)	60,702,855–60,697,398 (5,457)	323.7–329.4
6-19	60,473,559–60,467,459 (6,100)	60,744,773–60,738,593 (6,180)	265.0–277.3
6-21	60,202,369–60,198,628 (3,741)	60,817,436–60,813,287 (4,149)	610.9–618.8
6-22	60,206,616–60,202,204 (4,412)	60,773,541–60,770,871 (2,670)	566.9–568.7
6-30	60,218,415–60,212,528 (5,887)	60,702,855–60,697,398 (5,457)	484.4 484.9
p-10	60,202,369–60,198,628 (3,741)	60,615,999–60,611,135 (4,864)	408.8–417.4
p-43	59,205,733–58,114,483 (1.09 Mb)	60,488,718–60,484,754 (3,694)	1.3–2.4 Mb (3.6 Mb by aCGH)
p-154	60,170,294–60,162,440 (7,854)	60,669,880–60,675,660 (5,780)	505.4–507.4
p-851	60,342,915–60,337,367 (5,548)	60,767,899–60,765,908 (1,701)	425.0–428.5

Chr., chromosome

deletion clones (clones 3-5, 3-16, 6-3, *p*-10, *p*-43, *p*-154, and *p*-851) and in the nondeleted control. All deletion clones still exhibited FRA3B breaks but at a significantly reduced frequency compared with the control (Fig. 4) ($P = 0.0001–0.05$). We could not determine whether small differences in location or size of deletions variably affected fragility of FRA3B because almost all deletion clones exhibited breakage frequencies that were not significantly different from each other. However, clone *p*-43, which contains the largest deletion spanning 3.6 Mb, including the entire distal portion of *FHIT*, had the lowest frequency of FRA3B breaks, a 14-fold reduction compared with the control (Fig. 4) ($P = 0.001$), suggesting that there is a correlation of increased deletion size with decreased fragility.

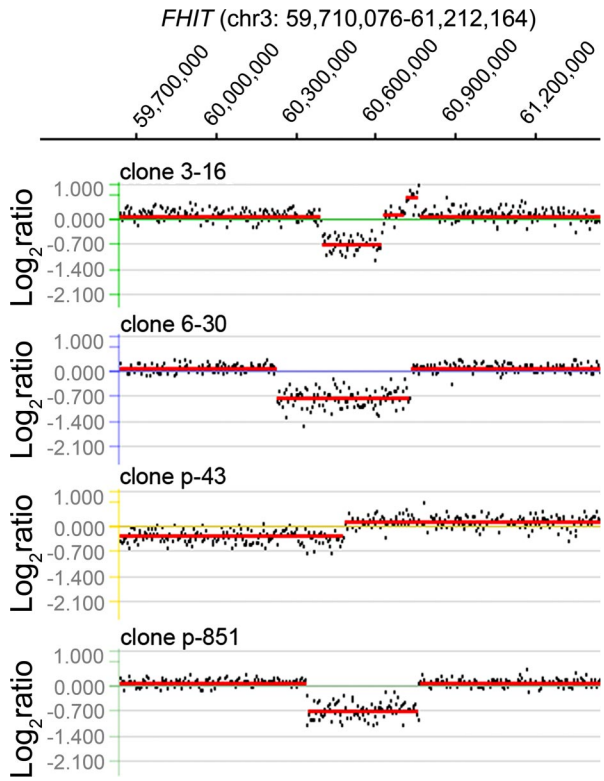

Fig. 2. aCGH analysis of deletion clones. aCGH plots showing submicroscopic deletions in four chromosome 3 somatic hybrid cell clones. The *y* axis indicates the log2 ratio of the reference DNA to the hybrid clone DNA. Copy number changes with log2 ratios >0.3 and <−0.3 were considered significant for duplicated or deleted sequences, respectively. The *x* axis indicates the genomic coordinates of each oligomer with respect to the *FHIT* gene, which spans chr3:59,710,076–61,212,164.

Analysis of Flexibility Peaks. Flexibility peaks, defined as regions with high local variations in twist angle have been hypothesized to play a role in CFS instability by generating unusual DNA structures that could impede replication (31). In an attempt to identify sequences that might contribute to FRA3B instability, we analyzed a conservative minimal deletion region, defined as any sequence deleted in two or more clones, and surrounding proximal and distal *FHIT* sequence, for flexibility peaks.

The minimal deletion region spanned 619 kb (60,817,436–60,198,628), the region of *FHIT* proximal to the minimal deletion region spanned 395 kb (61,212,164–60,817,436, and the region of *FHIT* distal to the minimal deletion region spanned 489 kb (60,198,627–59,710,076). By using the Twist Flex program to identify flexibility peaks, the 619-kb minimal deletion region was found to contain a total of 21 peaks exceeding the standard 13.7° threshold with an average flexibility of 10.98° (31) (SI Fig. 8*B* and SI Table 5). The regions of *FHIT* proximal and distal to the minimal deletion region contained a total of seven peaks and a flexibility averaging 10.93° and 16 peaks and an overall flexibility averaging 10.86°, respectively (SI Fig. 8 *A* and *C*, and SI Table 5). Thus, overall flexibility was virtually equivalent throughout *FHIT*. The minimal deletion region contains nearly twice the number of peaks per kilobase (1 peak per 29 kb) than the proximal segment of *FHIT* (1 peak every 56 kb) but nearly the same number of peaks per kilobase as the distal segment of *FHIT* (1 peak per 31 kb). These values are similar to the average incidence of flexibility peaks reported for both CFS and nonfragile regions of the human genome (1 peak per 24–32 kb) (32). No peaks were found to lie at predicted deletion boundaries, consistent with previously published studies that report that cancer-derived cell lines with *FHIT*/FRA3B deletions do not coincide with flexibility peaks (28).

Sequences at Deletion Breakpoints. At the 10- to 30-kb resolution used in the PCR screens, several clones appeared to share the same deletion boundaries that may represent hotspots for FRA3B breakage. The proximal deletion boundaries of clones 6-9, 6-11, and 6-30 mapped to the same 29-kb interval and were further refined to the same 5.5-kb interval by using additional PCR primers (Fig. 1 and Table 2). Five additional clones (3-1, 3-5, 6-9, 6-11, and 6-30) also shared proximal breakpoints mapping within a 12.8-kb region.

Table 3. Deletion breakpoints determined by aCGH

Clone	*FHIT* deletions		*FHIT* duplications
	Distal boundary	Proximal boundary	
6-30	60,230,237	60,734,018	None
p-851	60,342,988	60,765,820	None
p-43	56,889,623	60,487,704	None
3-16	60,401,085	60,627,358	60,716,2370–60,765,695

Because clones 6-9 and 6-11 originated from the same 0.6 μM APH-treated culture, it is possible that they represent a single, initial deletion derived from a common progenitor cell, with clone 6-11 acquiring a secondary proximal deletion. However, clone 6-30 was generated from a culture dish separate from clone 6-9 and 6-11. Thus, all three clones sharing this proximal breakpoint cannot have originated from a single cell that expanded before selection of clones. Similarly, clones 3-1 and 3-5, clones 6-9 and 6-11, and clone 6-30 were all generated from separate cultures and cannot have originated from expansion of a cell with a deletion in chromosome 3.

The distal deletion boundaries of clones 3-1 and 6-22, and clones 3-5 and 6-21, mapped to the same 4.4-kb interval (Fig. 1 and Table 2) and five clones (3-1, 3-5, 6-21, 6-22, and 6-30) shared distal breakpoints mapping within an 18.8-kb region (Table 2). As with clones sharing proximal deletion boundaries, clones 3-1 and 6-22 and clones 3-5 and 6-21 arose independently because they were generated from different culture dishes.

Using BLAST (www.ncbi.nlm.nih.gov/blast/bl2seq/wblast2.cgi), we found no regions of significant sequence similarity or sequence identity >10 nt between the proximal and distal breakpoint regions in 10 of the 15 deletion clones. In the other five clones, regions of identical sequence matches ranging from 13 to 43 nt were found. Thus, no extended stretches of sequence identity that would suggest homology-mediated repair were found in any of the breakpoint regions.

The high-resolution aCGH data allowed us to develop PCR primers mapping to within 2 kb of breakpoints and to amplify and sequence directly across the breakpoint junctions in three clones (3-16, 6-30, and *p*-851). We could not amplify across the breakpoint junction of the 3.6-Mb deletion in clone *p*-43, suggesting a complex rearrangement. To determine whether regions of homology were present at deletion breakpoints, we compared 2 kb of genomic sequence external to the deletion breakpoints and 10 kb internal to the deletion breakpoints in clones *p*-851, 6-30, and 3-16 by using the BLAST program. Based on pairwise comparison of the sequences present at the breakpoint regions, no direct or indirect repeats or identical sequences were found at the breakpoints, and no extended regions of homology or identical sequence >43 nt were found within these regions. In addition, we did not identify the presence of palindromic sequences in these regions by using the Human DNA Palindrome Database (HPALDB) (http://vhp.ntu.edu.sg/hpaldb). Rather, when we compared sequences across the breakpoint junctions to the sequences of the corresponding regions of the nondeleted control, which perfectly matched the human genome draft sequence, build 36.1. We observed a 3-bp ATT insertion in clone 6-30 (Fig. 5) and a 1-bp microhomology between breakpoints in clones 3-16 and *p*-851. These data are consistent with NHEJ-mediated repair at breakpoint junctions.

Discussion

FRA3B, which lies within the *FHIT* tumor-suppressor gene, is the most fragile locus in the human genome. Rearrangements and deletions of the *FHIT*/FRA3B locus are among the most common chromosome aberrations found in tumors and preneoplastic lesions. The fragile site-specific rearrangements most frequently observed are one or more large intralocus deletions of tens to hundreds of kilobases directly within the CFS region, often resulting in inactivation of the associated genes (16, 23–25, 28–30, 33–35). It has been hypothesized that CFS instability leads to these deletions after the formation of DNA DSBs upon exposure to replication stress (24, 25). However, almost all experimental studies of CFS instability have focused on factors influencing microscopically detectable CFS gaps and breaks on metaphase chromosomes, the biological significance of which could only be postulated. Although CFS instability has been shown to give rise to gross chromosomal aberrations including translocations and terminal deletions of 3p (1, 8) few translocations or gross rearrangements involving *FHIT*/FRA3B have been observed in tumor cells, and there has been no direct evidence demonstrating that CFS instability or replication stress can produce submicroscopic intralocus deletions of hundreds of kilobases at CFSs or elsewhere in the genome of any organism.

We have shown that *FHIT* deletions of hundreds of kilobases are induced at a high frequency by exposing chromosome 3

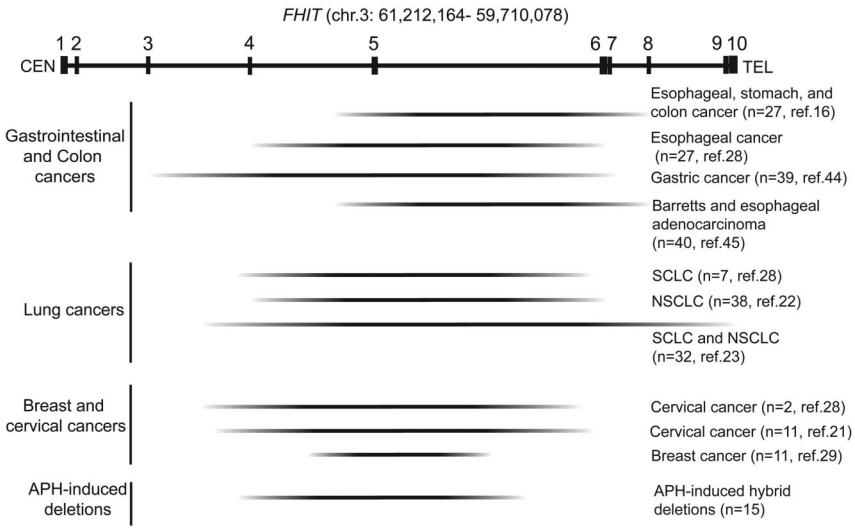

Fig. 3. *FHIT* deletions in human cancer. Representative examples of published deletions in cancers and cancer cell lines compared with APH-induced deletions. Each horizontal line represents regions deleted in >25% of ''*n*'' samples analyzed. Numbers in parentheses represent number of samples tested (*n*) and reference.

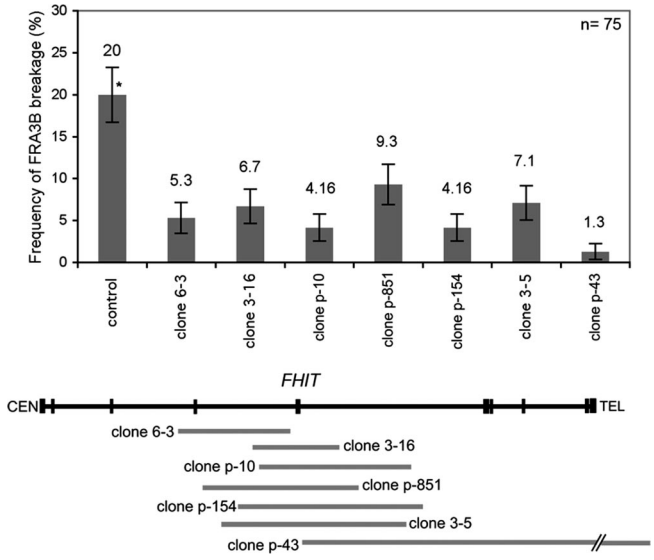

Fig. 4. FISH analysis of *FHIT*/FRA3B deletions. Frequency (%) of gaps and breaks at FRA3B in hybrid clones after 24-h APH treatment; $n = 100$ sites examined. Frequency of fragile-site breakage is presented as the percentage of chromosome 3s with breaks at FRA3B. Data were normalized with respect to total chromosome gaps and breaks to eliminate variability in cellular response to APH from clone to clone. All error bars indicate the 95% confidence interval. Locations of deletions in hybrid clones with respect to FHIT exons are shown as horizontal gray bars in the map. Clones are listed from smallest to largest deletion size. *, Numbers of FRA3B breaks in hybrid clones with deletions are significantly different from control hybrid cell lines ($P = 0.006$, 0.014, 0.002, 0.05, 0.002, 0.014, and 0.001 for clones 6-3, 3-16, *p*-10, *p*-154, 3-5, and *p*-43, respectively.

Fig. 5. Breakpoint junction sequences in clones 6-30, 3-16, and *p*-851. Sequences present at breakpoints are in uppercase and deleted sequences are in lowercase. Numerical positions of the breakpoints relative to the human genome draft sequence (hg18) are indicated. Microhomologies and 3-bp insertion at breakpoints are bold and underlined.

human–mouse somatic cell hybrids to APH-mediated replication stress. Each deletion was unique, although several deletion clones shared breakpoints mapping within intervals of 12–20 kb. The APH-induced deletions are similar to published *FHIT*/*FRA3B* tumor deletions in several respects. Like tumor deletions, the hybrid deletions span hundreds of kilobases within the *FHIT* gene. Furthermore, whereas exact sequences at *FHIT*/*FRA3B* tumor deletion breakpoints have not been defined, both APH-induced hybrid and many tumor *FHIT* deletions center on what is considered to be the midpoint of FRA3B fragility spanning *FHIT* introns 4 and 5 (22, 28, 29).

The *FHIT*/FRA3B deletions generated here are valuable reagents to study the contribution of DNA sequence to genome instability at CFSs. The exact sequences that confer CFS instability remain unidentified although several hypotheses have been proposed including increased incidence of flexibility peaks, repetitive elements, and AT-repeats (31, 36, 37). Based on TwistFlex analysis, *FHIT* was found to contain a total of 44 flexibility peaks. Although the minimal deletion region was found to have the greatest number of flexibility peaks per kilobase, mean flexibility was virtually equivalent throughout *FHIT*. When deletion clones were assayed for APH-induced FRA3B breakage, all still exhibited FRA3B breaks but at significantly reduced levels compared with undeleted control cells. Clone *p*-43, which contained the largest deletion spanning 37 of the 44 flexibility peaks within *FHIT*, showed the greatest reduction in FRA3B breakage. Because individual peaks with high degrees of flexibility were deleted in all hybrid clones, individual flexibility peaks are unlikely to be the sole feature responsible for CFS instability as assayed by metaphase chromosome gaps and breaks. It is more likely that multiple sequences or chromosomal features such as chromatin conformation within FRA3B collectively contribute to its instability.

The molecular mechanisms leading to APH-induced submicroscopic FRA3B deletions in cultured cells and in cancer cells are unknown. Although numerous investigations have focused on mechanisms of DNA DSB repair, nucleotide changes, small (<1 kb) deletions and gross chromosomal rearrangements, deletions, and duplications of the size we have seen at FRA3B have not previously been recognized as a consequence of replication stress in mammalian cells, or cells from any organism. This is likely because deletions of this size would not be well tolerated in bacteria or yeast and have not been detected in mammalian cells because of limitations in the methods of analysis. However, the cellular repair mechanisms involved in preventing and generating these deletions and duplications could be the same as those shown to function in generating smaller deletions. Previous studies have firmly linked stability of CFSs to the ATR-dependent cell cycle checkpoint response to stalled replication in mammalian cells (4). Stalled replication forks can collapse, leading to the formation of a DNA DSB (38). Deletions can result from DNA double-strand breaks that are repaired via homology-mediated pathways or by nonhomologous end joining (NHEJ). It has long been hypothesized, based on the coincident locations of SCEs at CFSs, that homologous recombination repair (HRR) is a likely candidate for repairing CFS lesions (8). More recently, data supporting a role for both NHEJ and HRR pathways in repair of CFS metaphase chromosome breaks have been reported (39).

The experiments described here have allowed us to begin to investigate specific sequences that may lead to CFS breakage and the mechanisms by which large deletions in these regions are formed. PCR data revealed that several FRA3B deletion clones shared breakpoints falling in close proximity to one another. Therefore, these sites may represent hotspots for instability. However, we were unable to correlate breakpoints with flexibility peaks, palindromic sequence, histone modifications (40) or extended regions of homology that might be responsible for breakage susceptibility in these regions. aCGH data allowed us to directly sequence the breakpoint junctions of three deletions. Analysis of 12 kb of sequence spanning the deletion breakpoints of these three clones did not reveal regions of homology or direct repeats, which would indicate homology-mediated repair through an unequal sister chromatid exchange event or single-strand annealing. Rather, we observed 1 bp of microhomology at the breakpoints of two clones and a 3-bp insertion in the third clone. Thus, it seems likely that NHEJ, or the related microhomology-mediated end-joining pathway (41) is responsible for repair of some CFS lesions leading to submicroscopic deletions at CFSs. Interestingly, one of four clones examined by aCGH showed a partial duplication in the FRA3B region, suggesting an unequal exchange event or other mechanism of repair in response to some lesions.

In summary, we have shown that APH-mediated replication stress reproducibly induces submicroscopic microdeletions spanning hundreds of kilobases within *FHIT*/FRA3B. These results

strongly support the hypothesis that replication stress during tumor formation contributes to deletions, and perhaps duplications, at CFSs that may inactivate associated tumor-suppressor genes such as FHIT. Thus, submicroscopic deletion may be a common result of replication stress. Furthermore, our approach provides a biologically relevant assay for studying CFS instability and for studies of factors that influence genomic rearrangements at CFSs, and elsewhere in the genome, after replication stress.

Materials and Methods

Generation of Deletion Clones. GM11713 human–mouse somatic cell hybrids were obtained from Coriell Cell Repository. Hybrid cells were maintained in DMEM media supplemented with 250 μg/ml active G418 (GIBCO) and 15% FBS. The integration site of the neo^r gene used for selection of chromosome 3 was determined by inverse PCR (described in ref. 42). To induce deletions, cells were treated with low doses (0.3 μM and 0.6 μM) of APH that still allow cells to divide and that are in the range of APH concentrations determined to be optimal for inducing metaphase CFS breaks in these cells. Cells were treated for 5 days, followed by a 1-day recovery period. Cells were then plated at a low density (100 cells per 100-mm culture dish). After 7–10 days, individual clones were isolated by using cloning rings. Thirty clones were selected at each dose of APH in addition to 30 untreated clones. Two cultures were treated at each dose level to ensure that any recurrent deletions did not arise from the same original cell.

PCR Detection of Genomic Deletions. Total genomic DNA was extracted by using the GentraPrep Puregene DNA Purification kit. PCR primers were designed by using Primer3 (http://frodo.wi.mit.edu/primer3/input.htm). One hundred forty-six markers spanning *FHIT*/FRA3B were analyzed by PCR, including markers in exons 1–10 of *FHIT* and loci flanking the *FHIT* gene. All primers are listed in SI Table 4. Primers were generated based on sequence from National Center for Biotechnology Information Build 36.1/hg18. PCRs were carried out in 25 μl containing 10 mM Tris·HCl), 50 mM KCl, 1.5 mM MgCl2, 200 μM deoxynucleotide triphosphates, 1.25 units of Taq polymerase, 0.2 μM final concentration of each primer, and $\approx$200 ng of DNA. PCR conditions consisted of an initial denaturation at 94°C for 3 min, followed by 30 cycles of denaturation at 94°C for 45 s, annealing at an optimized temperature between 58°C and 63°C for 45 s, and an extension at 65°C for 45 s, with a final extension at 72°C for 5 min. The amplified products were separated on 1.8% agarose gels and visualized by ethidium bromide staining.

Metaphase Chromosome and FISH Analysis. To induce CFS breaks, cells were treated with 0.8 μM APH for 24 h. Metaphase spreads were prepared and analyzed by FISH with the FRA3B-spanning YAC probe 850A6. Harvesting of cells, chromosome preparations, and FISH protocols were performed as described (19). Digoxigenin-labeled fosmids lying within FRA3B (WIBR2-1588A06, WIBR2-15211A22) and biotin-labeled control fosmids 5-Mb telomeric to FRA3B (WIBR2-2244H18) were used as probes to confirm FRA3B deletions.

aCGH. Chromosome 3 custom arrays containing 385,000 unique sequence oligonucleotides spaced at 110-bp intervals were obtained from Nimblegen Systems. Arrays were prepared according to the manufacturer's protocol. Arrays were scanned on an Axon 4000B scanner (Molecular Devices) with GenePlx software at 532 and 635 wavelengths. Data extraction normalization and visualization were achieved by using manufacturer-provided software (NimbleScan and SignalMap). Arrays were analyzed for copy number differences by using two algorithms: SegMNT, part of the NimbleScan software package provided by Nimblegen, and the R software module GLAD (43). Copy number differences detected by each software package were manually curated to include only variants with an average log2 ratio of more than 0.3 or less than -0.3, corresponding to a minimum change of at least 25% between test and reference.

Sequence Analysis. The TwistFlex program (http://bioinfo.md.huji.ac.il/marg/Flexstab) was used to analyze DNA flexibility [Mishmar *et al.* (31) and Kerem *et al.* (46). Default values were set for window size (100 bp), leap (1 bp), normalization value (10,000 bp), and threshold value (13.7°). The StabFlex program (http://home.gna.org/stabflex), based on the same algorithm as TwistFlex, was used to graph flexibility peaks.

Statistical Analysis. Total chromosome gaps and breaks data were analyzed by using Student's *t* test for equal or unequal variance. Variance was determined by using the sample variance *F* test. Fisher's two-sided exact test was used for analysis of specific CFS breakage.

ACKNOWLEDGMENTS. We thank Jose Garcia-Perez for help in mapping the neo^r insertion in GM11713 cells; Evan Eichler and James Sprague (University of Washington, Seattle) for the gift of WIBR2 library fosmid clones; John Moran, Thomas Wilson, and Niall Howlett for helpful comments; and Pembroke Davis for help in running the StabFlex analyses. This work was supported by National Institutes of Health Grant CA43222.

1. Glover TW, Berger C, Coyle J, Echo B (1984) *Hum Genet* 67:136–142.
2. Nagano H, Ikegami S (1980) *Seikagaku* 52:1208–1216.
3. Arlt MF, Xu B, Durkin SG, Casper AM, Kastan MB, Glover TW (2004) *Mol Cell Biol* 24:6701–6709.
4. Casper AM, Nghiem P, Arlt MF, Glover TW (2002) *Cell* 111:779–789.
5. Durkin SG, Arlt MF, Howlett NG, Glover TW (2006) *Oncogene* 25:4381–4389.
6. Howlett NG, Taniguchi T, Durkin SG, D'Andrea AD, Glover TW (2005) *Hum Mol Genet* 14:693–701.
7. Glover TW, Stein CK (1987) *Am J Hum Genet* 41:882–890.
8. Glover TW, Stein CK (1988) *Am J Hum Genet* 43:265–273.
9. Wang ND, Testa JR, Smith DI (1993) *Genomics* 17:341–347.
10. Fechter A, Buettel I, Kuehnel E, Schwab M, Savelyeva L (2007) *Int J Cancer* 120:2359–2367.
11. Rassool FV, McKeithan TW, Neilly ME, van Melle E, Espinosa R, III, Le Beau MM (1991) *Proc Natl Acad Sci USA* 88:6657–6661.
12. Thorland EC, Myers SL, Persing DH, Sarkar G, McGovern RM, Gostout BS, Smith DI (2000) *Cancer Res* 60:5916–5921.
13. Coquelle A, Pipiras E, Toledo F, Buttin G, Debatisse M (1997) *Cell* 89:215–225.
14. Huebner K, Garrison PN, Barnes LD, Croce CM (1998) *Annu Rev Genet* 32:7–31.
15. O'Keefe LV, Richards RI (2006) *Cancer Lett* 232:37–47.
16. Ohta M, Inoue H, Cotticelli MG, Kastury K, Baffa R, Palazzo J, Siprashvili Z, Mori M, McCue P, Druck T, *et al.* (1996) *Cell* 84:587–597.
17. Bednarek AK, Laflin KJ, Daniel RL, Liao Q, Hawkins KA, Aldaz CM (2000) *Cancer Res* 60:2140–2145.
18. Boldog F, Gemmill R, West J, Robinson M, Li E (1997) *Hum Mol Genet* 6:193–203.
19. Wilke CM, Hall BK, Hoge A, Paradee W, Smith DI, Glover TW (1996) *Hum Mol Genet* 5:187–195.
20. Arlt MF, Durkin SG, Ragland RL, Glover TW (2006) *DNA Repair* 5:1126–1135.
21. Corbin S, Neilly ME, Espinosa R, III, Davis EM, McKeithan TW, Le Beau MM (2002) *Cancer Res* 62:3477–3484.
22. Li R, Todd NW, Qiu Q, Fan T, Zhao RY, Rodgers WH, Fang HB, Katz RL, Stass SA, Jiang F (2007) *Clin Cancer Res* 13:482–487.
23. Sozzi G, Veronese ML, Negrini M, Baffa R, Cotticelli MG, Inoue H, Tornielli S, Pilotti S, De Gregorio L, Pastorino U, *et al.* (1996) *Cell* 85:7–26.
24. Bartkova J, Horejsi Z, Koed K, Kramer A, Tort F, Zieger K, Guldberg P, Sehested M, Nesland JM, Lukas C, *et al.* (2005) *Nature* 434:864–870.
25. Gorgoulis VG, Vassiliou LV, Karakaidos P, Zacharatos P, Kotsinas A, Liloglou T, Venere M, Ditullio Jr. RA, Kastrinakis NG, Levy B, *et al.* (2005) *Nature* 434:907–913.
26. Lai LA, Paulson TG, Li X, Sanchez CA, Maley C, Odze RD, Reid BJ, Rabinovitch PS (2007) *Genes Chrom Cancer* 46:532–542.
27. Ning Y, Lovell M, Taylor L, Pereira-Smith OM (1992) *Cytogenet Cell Genet* 60:79–80.
28. Mimori K, Druck T, Inoue H, Alder H, Berk L, Mori M, Huebner K, Croce CM (1999) *Proc Natl Acad Sci USA* 96:7456–7461.
29. Negrini M, Monaco C, Vorechovsky I, Ohta M, Druck T, Baffa R, Huebner K, Croce CM (1996) *Cancer Res* 56:3173–3179.
30. Kastury K, Baffa R, Druck T, Ohta M, Cotticelli MG, Inoue H, Negrini M, Rugge M, Huang D, Croce CM, *et al.* (1996) *Cancer Res* 56:978–983.
31. Mishmar D, Rahat A, Scherer SW, Nyakatura G, Hinzmann B, Kohwi Y, Mandel-Gutfroint Y, Lee JR, Drescher B, Sas DE, *et al.* (1998) *Proc Natl Acad Sci USA* 95:8141–8146.
32. Helmrich A, Stout-Weider K, Hermann K, Schrock E, Heiden T (2006) *Genome Res* 16:1222–1230.
33. Boldog FL, Waggoner B, Glover TW, Chumakov I, Le Paslier D, Cohen D, Gemmill RM, Drabkin HA (1994) *Genes Chrom Cancer* 11:216–221.
34. Druck T, Hadaczek P, Fu T-B, Ohta M, Siprashvili Z, Baffa R, Negrini M, Kastury K, Veronese ML, Rosen D, *et al.* (1997) *Cancer Res* 57:504–512.
35. Ong ST, Fong KM, Bader SA, Minna JD, Le Beau MM, McKeithan TW, Rassool FV (1997) *Genes Chromosomes Cancer* 20:16–23.
36. Morelli C, Karayianni E, Magnanini C, Mungall AJ, Thorland E, Negrini M, Smith DI, Barbanti-Brodano G (2002) *Oncogene* 21:7266–7276.
37. Ried K, Finnis M, Hobson L, Mangelsdorf M, Sayan S, Nancarrow JK, Woollatt E, Kremmidiotis G, Gardner A, Venter D, *et al.* (2000) *Hum Mol Genet* 9:1651–1663.
38. Higgins NP, Kato K, Strauss B (1976) *J Mol Biol* 101:417–425.
39. Schwartz M, Zlotorynski E, Goldberg M, Ozeri E, Rahat A, le Sage C, Chen BP, Chen DJ, Agami R, Kerem B (2005) *Gen Dev* 19:2715–2726.
40. Barski A, Cuddapah S, Cui K, Roh TY, Schones DE, Wang Z, Wei G, Chepelev I, Zhao K (2007) *Cell* 129:823–837.
41. Liang L, Deng L, Chen Y, Li GC, Shao C, Tischfield JA (2005) *J Biol Chem* 280:31442–31449.
42. Ochman H, Gerber AS, Hartl DL (1988) *Genetics* 120:621–623.
43. Hupe P, Stransky N, Thiery JP, Radvanyi F, Barillot E (2004) *Bioinformatics* 20:3413–3422.
44. Huiping C, Kristjansdottir S, Bergthorsson JT, Jonasson JG, Magnusson J, Egilsson V, Ingvarsson S (2002) *Eur J Cancer* 38:728–735.
45. Michael D, Beer DG, Wilke CW, Miller DE, Glover TW (1997) *Oncogene* 15:1653–1659.
46. Zlotorynski E, Rahat A, Skaug J, Ben-Porat N, Ozeri E, Hershberg R, Levi A, Scherer SW, Margalit H, Kerem B (2003) *Mol Cell Biol* 23:7143–7151.